Pairing state in the ruthenocuprate superconductor $RuSr_2GdCu_2O_8$: A point-contact Andreev reflection spectroscopy study

Samanta Piano, Fabrizio Bobba, Filippo Giubileo, Anna Maria Cucolo, Marcello Gombos, and Antonio Vecchione
Physics Department and INFM-CNR SUPERMAT Laboratory, University of Salerno, Via S. Allende, 84081 Baronissi (SA), Italy
(Received 10 September 2005; revised manuscript received 18 November 2005; published 21 February 2006)

The results of point contact Andreev reflection spectroscopy on polycrystalline $RuSr_2GdCu_2O_8$ pellets are presented. The wide variety of the measured spectra are all explained in terms of a modified Blonder–Tinkham–Klapwijk model considering a *d-wave* symmetry of the superconducting order parameter. Remarkably low values of the energy gap $\Delta=(2.8\pm0.2)$ meV and of the $2\Delta/k_BT_c\simeq2$ ratio are inferred. From the temperature evolution of the dI/dV vs V characteristics we extract a sublinear temperature dependence of the superconducting energy gap. The magnetic field dependence of the conductance spectra at low temperatures is also reported. From the Δ vs H evolution, a critical magnetic field $H_{c_2}\simeq30$ T is inferred. To properly explain the curves showing gap-like features at higher voltages, we consider the formation of a Josephson junction in series with the point contact junction, as a consequence of the granularity of the sample.

DOI: 10.1103/PhysRevB.73.064514 PACS number(s): 74.50.+r, 74.45.+c, 74.20.Rp, 74.72.−h

I. INTRODUCTION

Point contact spectroscopy[1] is a versatile technique widely used to study the basic properties of superconductors, such as the density of states at the Fermi level and the superconducting energy gap. The technique consists in establishing a contact between a tip of a normal metal (N) and a superconducting sample (S), thus forming a small contact area that is a "point contact" junction. By varying the distance and/or the pressure between tip and sample it is possible to obtain different tunnel barriers, that is, different conductance regimes. Indeed, quasiparticle tunnel spectroscopy is obtained for high barriers, while point contact Andreev reflection (PCAR) spectroscopy is achieved in case of low barriers. Often in the experiments, intermediate regimes are realized, in which through the N/S contact both quasiparticle tunneling and Andreev reflection processes occur.

Andreev reflections[2,3] take place at the N/S interface when an electron, propagating in the normal metal with an energy lower than the superconducting energy gap, enters in the superconductor forming an electron pair (Cooper pair) while a hole, with opposite momentum with respect to the incident electron, is reflected in the normal metal. A single reflection corresponds to a net charge transfer of $2e$, where e is the electron charge, from the normal metal to the superconductor. In the limit of low barriers at low temperatures, all the incident electrons at the N/S interface with energy $eV<\Delta$ are Andreev reflected and the conductance doubles the normal states value.

In this paper we report on PCAR studies carried out in the hybrid rutheno-cuprate $RuSr_2GdCu_2O_8$ (Ru-1212) system.[4] This compound has recently drawn great attention among theorists and experimentalists in the field of solid state physics due to the coexistence at low temperatures of superconducting and magnetic ordering.[5] The Ru-1212 structure is similar to that of $YBa_2Cu_3O_7$ with magnetic (two-dimensional) RuO_2 planes substituting the (one-dimensional) Cu–O chains. The superconducting critical temperature in this compound strongly depends on the preparation conditions with some reports showing transition onset as high as 50 K.[6] The Ru-1212 also shows a magnetic phase below 135 K. It has been reported that the magnetic order of the Ru moments is predominantly antiferromagnetic along the c axis,[7] while a ferromagnetic component has been observed in the RuO_2 planes, that act as charge reservoir.[8] At the moment, due to complexity of this compound, an exhaustive description of the interaction between the magnetic and superconducting layers is still missing as well as an unambiguous evaluation of the symmetry of the energy gap.

The paper is organized as follows: in Sec. II we briefly review the results of the Blonder–Tinkham–Klapwijk (BTK) model[9] for a conventional *s-wave* superconductor and the recent extensions[10] for anisotropic *s-wave* and *d-wave* symmetry of the order parameter. In Sec. III we describe the point contact experiments in polycrystalline Ru-1212 pellets showing a variety of conductance curves obtained at $T=4.2$ K. Satisfactory theoretical fittings are achieved by using a modified BTK model for *d-wave* symmetry of the order parameter. In Sec. IV we show that, due to the granularity of the samples, in some cases, the formation of a Josephson junction in series with the N/S contact occurs. Indeed, conductance curves showing gap-like features at higher voltages and dips in the spectra are well explained by this assumption. In Sec. V we report the temperature evolution of the conductance curves of a very stable junction. All the spectra are well reproduced by the *d-wave* modified BTK model, and we infer from the experiments the temperature dependence of the superconducting energy gap Δ. In Sec. VI we analyze the magnetic field behavior of the measured conductance spectra, providing an estimation of the upper critical field of the Ru-1212 compound. Finally, in Sec. VII we summarize our results and draw some conclusions.

II. BTK MODEL AND ITS EXTENSION

In this section, for sake of clearness, we review the main results of the original BTK theoretical model,[9] as developed for electronic transport through a point-contact junction be-

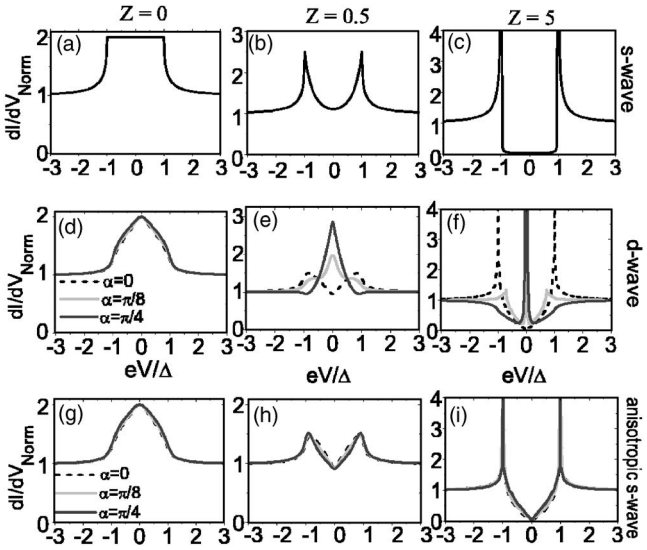

FIG. 1. Conductance characteristics, at low temperatures, for different barriers Z as obtained by the BTK model for a point contact junction between a normal metal and a *s-swave* [(a),(b),(c)], a *d-swave* [(d),(e),(f)] and an anisotropic *s-wave* superconductor [(g),(h),(i)].

tween a normal metal and a conventional Bardeen–Cooper–Schrieffer (BCS) superconductor. We also summarize the Kashiwaya–Tanaka[10] extension for asymmetric *s-wave* and *d-wave* superconductors. Indeed, a close comparison of the calculated conductance spectra is useful for a better understanding of the peculiar transport processes that occur at an N/S interface depending on the symmetry of the superconducting order parameter.

Following the original paper, we write the expression of the differential conductance characteristics for a N/S contact that, according to the BTK model,[9] is given by

$$G_{NS}(\mathrm{eV}) = \frac{dI(\mathrm{eV})}{dV} = G_{NN}\int_{-\infty}^{+\infty} dE[1 + A(E) - B(E)] \times \left[-\frac{df(E+\mathrm{eV})}{d(\mathrm{eV})}\right] \tag{1}$$

where eV is the applied potential, $G_{NN}=4/(4+Z^2)$ is the normal conductance expressed in terms of Z, a dimensionless parameter modeling the barrier strength, $f(E)$ is the Fermi function and $A(E)$ and $B(E)$ are, respectively, the Andreev reflection and normal reflection probabilities for an electron approaching the N/S interface. Equation (1) shows that, while ordinary reflections reduce the transport current through the junction, Andreev reflections increase this by transferring two electrons (Cooper pair) in the superconducting electrode on the other side of the barrier. The case $Z=0$ corresponds to a completely transparent barrier so that the transport current is predominantly due to Andreev reflections and $G_{NS}(V<\Delta)/G_{NN}(V\gg\Delta)=2$ is found [Fig. 1(a)]. By increasing Z, the Andreev reflections are partially suppressed and the conductance spectra tend to the case of a N/I/S tunnel junction showing peaks at $eV=\pm\Delta$ [Figs. 1(b) and 1(c)].

Recently, Kashiwaya and Tanaka[10] extended the BTK model by considering different symmetries of the order parameter. Indeed, for a *d-wave* superconductor, the electron-like and hole-like quasiparticles, incident at the N/S interface, experience different signs of the order parameter, with formation of Andreev bound states at the Fermi level along the nodal directions. The presence of Andreev bound states modifies the transport current and the expression of the differential conductance is given by

$$G_{NS}(V) = \frac{\displaystyle\int_{-\infty}^{+\infty} dE \int_{-\pi/2}^{+\pi/2} d\varphi \sigma(E,\varphi)\cos\varphi \left[-\frac{df(E+eV)}{d(eV)}\right]}{\displaystyle\int_{-\infty}^{+\infty} dE\left[-\frac{df(E+eV)}{d(eV)}\right]\int_{-\pi/2}^{+\pi/2} d\varphi \sigma_N(\varphi)\cos(\varphi)}, \tag{2}$$

where

$$\sigma(E,\varphi) = \sigma_N(\varphi)\frac{[1+\sigma_N(\varphi)]\Gamma_+^2 + (\sigma_N(\varphi)-1)(\Gamma_+\Gamma_-)^2}{(1+(\sigma_N(\varphi)-1)\Gamma_+\Gamma_-)^2} \tag{3}$$

is the differential conductance and

$$\sigma_N(\varphi) = \frac{1}{1+\tilde{Z}(\varphi)^2}, \quad \tilde{Z}(\varphi) = Z\cos(\varphi), \tag{4}$$

$$\Gamma_\pm = \frac{E - \sqrt{E^2 - \Delta_\pm^2}}{\Delta_\pm}, \tag{5}$$

$$\Delta_\pm = \Delta\cos[2(\alpha \mp \varphi)]. \tag{6}$$

So, at a given energy E, the transport current depends both on the incident angle φ of the electrons at the N/S interface as well as on the orientation angle α, that is, the angle between the *a axis* of the superconducting order parameter and the *x axis*. When applying Eqs. (2)–(6) to PCAR experiments, there is no preferential direction of the quasiparticle injection angle φ into the superconductor, so the transport current results by integration over all directions inside a semisphere weighted by the scattering probability term in the current expression. Moreover, because our experiments deal with polycrystalline samples, the angle α is a pure average fitting parameter, which depends on the experimental configuration.

In case of *d-wave* symmetry, for $Z\to 0$, the conductance curves at low temperatures show a triangular structure centered at $eV=0$, quite insensitive to variations of α with maximum amplitude $G_{NS}(V=0)/G_{NN}(V\gg\Delta)=2$ [Fig. 1(d)]. However, for higher barriers, the conductance characteristics show dramatic changes as function of α. In particular, as soon as $\alpha\neq 0$, the presence of Andreev bound states at the Fermi level produces strong effects more evident along the nodal direction ($\alpha=\pi/4$) for which $G_{NS}(V=0)/G_{NN}(V\gg\Delta) > 2$ is found [Figs. 1(e) and 1(f)].

For comparison, we report the conductance behavior for anisotropic *s-wave* superconductor, in which only the amplitude of the order parameter varies in the k space, while the phase remains constant and Eq. (6) reduces to

$$\Delta_+ = \Delta_- = \Delta \cos[2(\alpha - \varphi)]. \quad (7)$$

Again, in the limit $Z \to 0$, an increase of the conductance for $E < \Delta$ with a triangular profile is found with maximum amplitude $G_{NS}(V=0)/G_{NN}(V \gg \Delta)=2$ at zero bias [Fig. 1(g)]. On the other hand, for higher Z, we obtain tunneling conductance spectra that show the characteristic "V"-shaped profile in comparison to the classical "U"-shaped structure found for an isotropic *s-wave* order parameter [Figs. 1(h) and 1(i)]. We notice that in this case all the curves are quite insensitive to variation of the α parameter and a zero bias peak is obtained only for low barriers.

III. PCAR SPECTROSCOPY ON $RuSr_2GdCu_2O_8$: EXPERIMENTS AND THEORETICAL FITTINGS

The Ru-1212 samples used for this study were directionally solidified pellets, grown by means of the top-seeded melt-textured method starting from Ru-1212 and Ru-1210 ($RuSr_2GdO_6$) powder mixtures with a ratio Ru-1212/Ru-1210=0.2. The details of the preparation procedure are reported elsewhere.[11] In the x-ray diffraction patterns, a single Ru-1212 phase was found. In the resistivity measurements versus temperature, the onset of the superconducting transition was observed at $T_c^{on} \simeq 43$ K with $T_c(\rho=0) \simeq 24$ K and $\Delta T_c = 12$ K (ΔT_c is defined as the difference between the temperatures measured at 90% and 10% of the normal state resistance). We notice that a broadening of the superconducting transition is often observed in polycrystalline samples and it is usually related to the formation of intergrain weak Josephson junctions.[5,12,13] We address this point in the next section.

To realize our experiments we used a Pt–Ir tip, chemically etched in a 40% solution of HCl, while Ru-1212 samples were cleaned in an ultrasound bath in ethyl alcohol. Sample and tip were introduced in the PCAR probe, in which three micrometric screws are allocated, each driven by its own crank. Two screws allow to vary the distance between tip and sample, with a precision of 1 and 0.1 μm, respectively. The third screw is devoted to change the inclination of the sample holder varying the contact area on the sample surface. The point contact junctions were formed by pushing the Pt–Ir tip on the Ru-1212 pellet surface with the probe thermalized in the liquid He^4 bath. The current-voltage (I vs V) characteristics were measured by using a conventional four-probe method and a lock-in technique with an amplitude of the ac current less than 1 μA was used to measure the differential conductance (dI/dV vs V) spectra as function of the applied voltage.

In Fig. 2, we show a variety of normalized conductance spectra obtained at $T=4.2$ K by establishing different contacts on different areas of the same Ru-1212 pellet. The junction resistances varied between 10 and 100 Ω. By using the Sharvin relation,[14] it has been possible to achieve an estimation of the size of the contact area. Indeed $R=\rho l/4a^2$, where $\rho=0.4$ mΩ cm is the low temperature resistivity and $l \approx 1000$ Å, as estimated in Ref. 11. In our case, we have found that the typical contact size varied between 300 and 1000 Å.

We observe that all the reported spectra are characterized by a zero bias conductance peak (ZBCP) with a triangular structure, the main features appearing for each contact with different shapes, amplitudes and energy widths. Quite often, oscillations are observed on the conductance background, as shown in Figs. 2(c)–2(f). We observe that the ZBCP appears as a simple structure in Fig. 2(b), while in the remaining spectra it results being structured with variations of slope or secondary maxima, as in Fig. 2(e). The maximum conductance ratio $G_{NS}(V=0)/G_{NN}(V \gg \Delta)$ is less than 2 for all the curves, however $G_{NS}(V=0)/G_{NN}(V \gg \Delta) \simeq 2.2$ for the data in Fig. 2(f). In addition to this, the energy width of the main zero bias triangular structure is lower than 10 mV in Figs. 2(a)–2(d) while it becomes wider, around 40 mV, in Figs. 2(e) and 2(f). At a first qualitative analysis, these data appear quite puzzling and could be interpreted in terms of local, large variations of the superconducting energy gap. In the following, we will show that the theoretical fittings of all the spectra give a clear indication of a *d-wave* symmetry of the superconducting order parameter, with consistent values of the inferred amplitude of the energy gap.

First of all, let us quantitatively analyze the curves of Figs. 2(a)–2(d). We were not able to reproduce the conductance spectra reported in Figs. 2(a) and 2(b) by using either the conventional *s-wave* model or the anisotropic one, even by considering small Z values, indicative of low barriers. On the other hand, as can be observed in Fig. 1, the *s-wave* fittings cannot model the structured conductances reported in Figs. 2(c) and 2(d). The solid lines in the figures are the theoretical fittings obtained by considering a *d-wave* symmetry of the order parameter in the modified BTK model, Eqs. (2)–(6). A satisfactory agreement is obtained by using as fitting parameters the superconducting energy gap Δ, the barrier strength Z, the angle α and a phenomenological factor Γ^{Dynes}[15] to take into account pair breaking effects and finite quasiparticle lifetime.[16] We notice that in the considered spectra, both quasiparticle tunneling and Andreev reflection processes take place, since intermediate Z values have to be used to simulate the barrier strength ($0.45 \leqslant Z \leqslant 0.9$). Moreover, the angle α varies between 0.39 and 0.51, indicating that the average transport current mainly flows along an intermediate direction between the nodal one ($\alpha=\pi/4$) and that of the maximum amplitude of the energy gap ($\alpha=0$). The modified *d-wave* BTK model allows to satisfactorily reproduce the variations of slope around ±1 mV of the structured ZBCP in Figs. 2(a), 2(c), and 2(d) with a light discrepancy in modeling the full height of the peak in Fig. 2(d). We show in the next section that a more satisfactory fitting for this contact can be obtained by taking into account an additional in series intergrain junction.

We remark that the values of the superconducting energy gap, inferred from the theoretical fittings, are all consistent and enable us to estimate an average value of the amplitude of the order parameter $\Delta=(2.8 \pm 0.2)$ meV. This value is surprisingly low in comparison with the amplitude of the energy gap in other cuprate superconductors, however the possibility that the presence of the RuO_2 magnetic planes can play an important role in the complex Ru-1212 system has to be taken into account. We notice that the ratio between the

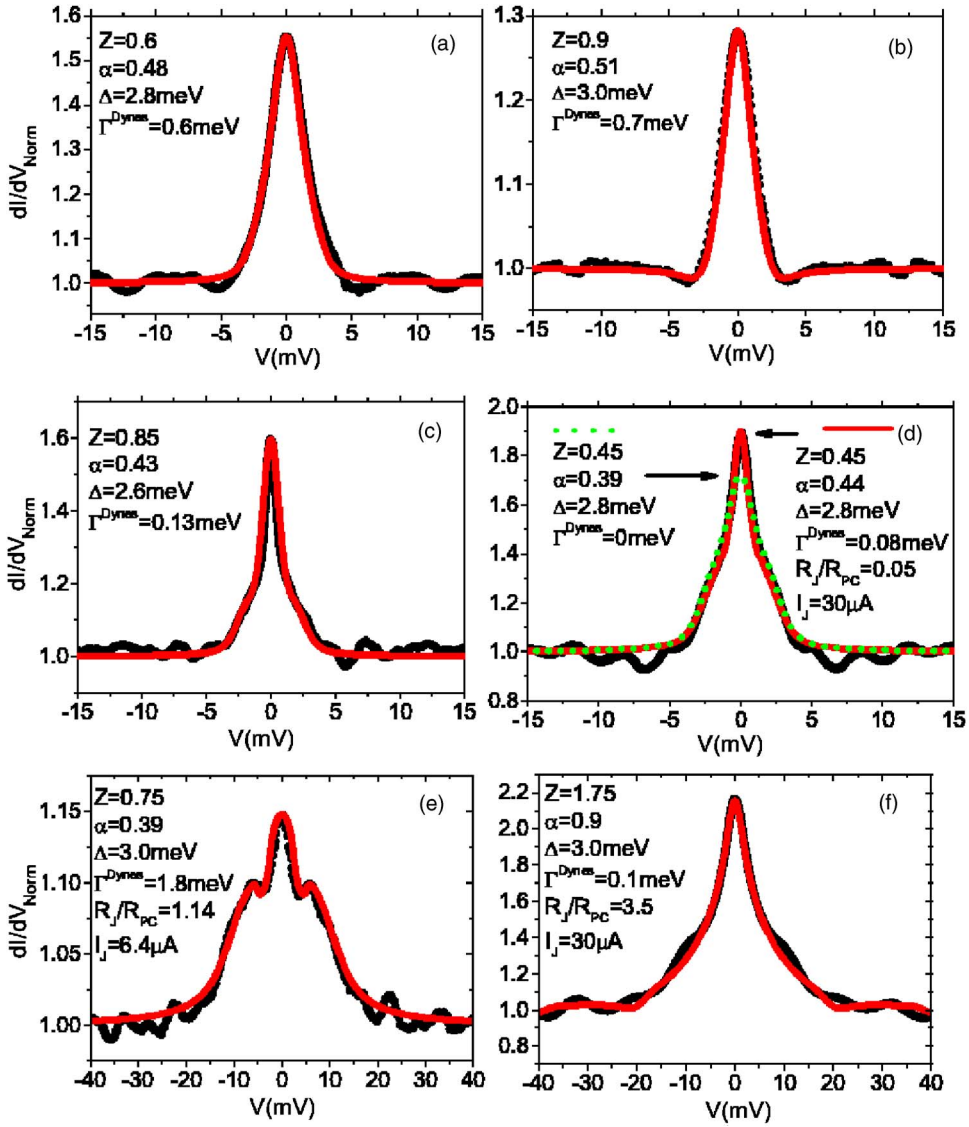

FIG. 2. (Color online) The dI/dV vs V characteristics measured in different Ru-1212/Pt–Ir PC junctions at 4.2 K. The experimental data (dots) are shown together with the best theoretical fittings (solid lines) obtained by a modified BTK model for a *d-wave* symmetry of the superconducting order parameter.

smearing factor Γ^{Dynes} and the superconducting energy gap is always less than 20% and it vanishes for the fitting shown in Fig. 2(d). We consider this fact as an indication of the good quality of our point contact junctions.

IV. ROLE OF THE INTERGRAIN COUPLING

To complete our discussion about the spectra measured at low temperatures, we now address the analysis of the conductance curves reported in Figs. 2(e) and 2(f), with a wider ZBCP. In this respect, we observe that, due to the granularity of the compound, in same cases, an intergrain Josephson junction can be formed in series with the point contact one, as schematically drawn in Fig. 3. This topic has been recently addressed in PCAR studies on $MgCNi_3$[17] and MgB_2.[18]

To provide a quantitative evaluation of the conductance spectra, we consider a real configuration in which the Pt–Ir tip realizes a point contact junction on a single Ru-1212 grain, which, in turn, is weakly coupled to another grain, so forming a Josephson junction. In this case the measured voltage corresponds to the sum of two terms

$$V_{\text{measured}}(I) = V_{PC}(I) + V_J(I), \tag{8}$$

where V_{PC} and V_J are the voltage drops at the N/S point contact junction and at the S/I/S intergrain Josephson junc-

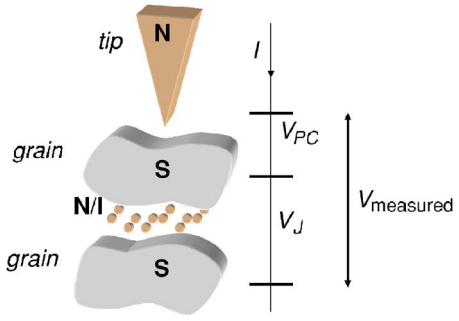

FIG. 3. (Color online) Intergrain coupling effect in polycrystalline samples. The measured voltage $V_{measured}$ is the sum of two terms: V_{PC}, the voltage drops between tip and sample, the N/S point contact junction, and V_J, the voltage drops between two superconducting grains, forming the S/I/S Josephson junction.

tion, respectively. This last contribution can be calculated by the Lee formula[19] which, in the limit of small capacitance and at low temperatures, reduces to the simplified expression[20]

$$V_J = \begin{cases} 0 & \text{for } I < I_J; \\ R_J I_J \sqrt{[(I/I_J)^2 - 1]} & \text{for } I \geqslant I_J. \end{cases} \quad (9)$$

At the same time, for the point contact contribution, we use again the extended BTK model for a *d-wave* superconductor. The $I(V)$ characteristic is then calculated by inverting Eq. (8) and the conductance spectrum is given by

$$\sigma(V) = \frac{dI}{dV} = \left(\frac{dV_{PC}}{dI} + \frac{dV_J}{dI} \right)^{-1}. \quad (10)$$

By applying this simple model we have satisfactory fitted the experimental data reported in Figs. 2(e) and 2(f). Remarkably, for both spectra, the best fittings have been obtained by using $\Delta = 3.0$ meV, consistently with the average value extracted from the other curves in Figs. 2(a)–2(d). We observe that, in this model, two more parameters are needed, namely the resistance R_J and the critical current I_J of the Josephson junction. However, the choice of these two parameters is not completely arbitrary, since the condition $R_J + R_{PC} = R_{NN}$ has to be fulfilled, where R_{NN} is the measured normal resistance and the product $R_J I_J$ necessarily results lower than Δ.[21]

In some cases, it has been pointed out that dips in the conductance spectra can be related to the presence of intergrain junctions,[17,18] and for sake of completeness, we have applied our model also to the spectra of Figs. 2(a)–2(d). We notice that for different junctions, the effect of the intergrain coupling is more or less evident, depending on ratio R_J/R_{PC}. For the conductances shown in Figs. 2(a)–2(c) this effect turns out to be negligible, however some improvement of the theoretical fitting is obtained in the case of Fig. 2(d) (see dashed line). Remarkably, by this last fitting we have found the same value of the superconducting energy gap previously inferred, $\Delta = 2.8$ meV, with a Γ^{Dynes}/Δ ratio less than 3% and $R_J/R_{PC} = 0.05$.

V. TEMPERATURE DEPENDENCE OF THE CONDUCTANCE SPECTRA

To achieve information on the temperature dependence of the superconducting energy gap in the Ru-1212 system, in this section we analyze the temperature behavior of the conductance spectrum shown in Fig. 2(d). Indeed, this PCAR junction became very stable for temperature variations.

In Fig. 4 we show the conductance characteristics measured in the temperature range $4.2K \leqslant T < 35$ K. We first notice that the ZBCP decreases for increasing temperature and disappears at about $T \simeq 30$ K, that we estimate as the local critical temperature T_c^l of the superconducting Ru-1212 grain in contact with the Pt–Ir tip, consistently with the resistivity measurements.[11] This fact provides further evidence that the ZBCP is a consequence of the superconducting nature of Ru-1212 and is not due to spurious effects like inelastic tunneling via localized magnetic moments in the barrier region.[22] The experimental data for each temperature are then compared to the theoretical fittings calculated by using the *d-wave* modified BTK model with a small contribution of Josephson junction in series. For all the curves, we fixed the strength of the barrier and the angle α to the values obtained at the lowest temperature.

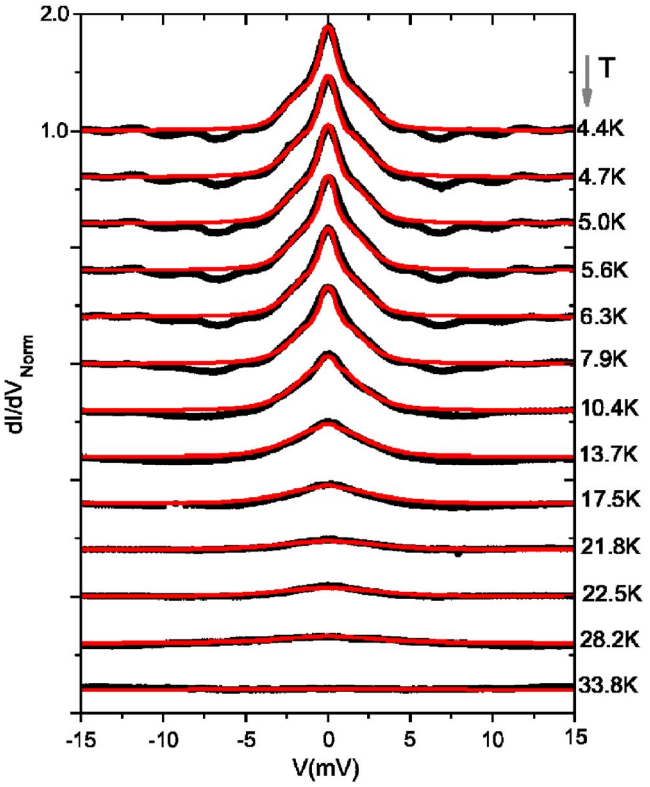

FIG. 4. (Color online) Temperature evolution of the conductance spectrum of Fig. 2(c) from $T = 4.2$ K to up the critical temperature (dots). The solid lines are the theoretical fittings obtained by a modified *d-wave* BTK model with the energy gap as only free parameter.

The resulting temperature dependence of the superconducting energy gap $\Delta(T)$ is reported in Fig. 5, where vertical bars indicate the errors in the gap amplitude evaluation, that increase when approaching the critical temperature. Contrarily to what is expected for BCS superconductors, we observe that the energy gap, at low temperatures, decreases rapidly for increasing temperatures and goes to zero at T_c^l in a sublinear way. We notice that the same temperature evolution for the superconducting energy gap is found trough the *d-wave* BTK model with or without considering any intergrain junction in series; remarkably, in this last case, the superconducting energy gap Δ remains the only varying parameter. A similar temperature dependence has been reported by Ummarino *et al.*,[23] however these authors give a larger estimation of the maximum gap amplitude.

From the average value of the superconducting energy gap $\Delta = 2.8$ meV and from the measured local critical temperature $T_c^l \simeq 30$ K, we obtain a ratio $2\Delta/(k_B T_c^l) \simeq 2$ much smaller than the predicted BCS value and also smaller than the values found for high-T_c cuprate superconductors.[24] Again we speculate that the simultaneous presence of super-

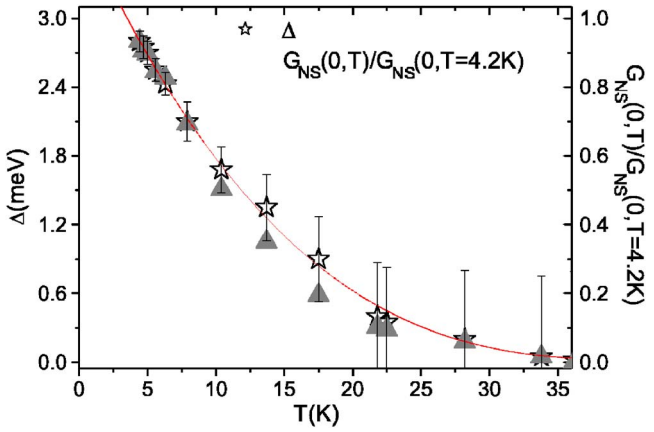

FIG. 5. (Color online) Temperature dependence of the superconducting energy gap as inferred from the theoretical fittings shown in Fig. 4. The solid line is a guide for the eyes. The right hand scale refers to the temperature evolution of the measured height of the ZBCP normalized to the 4.2 K value.

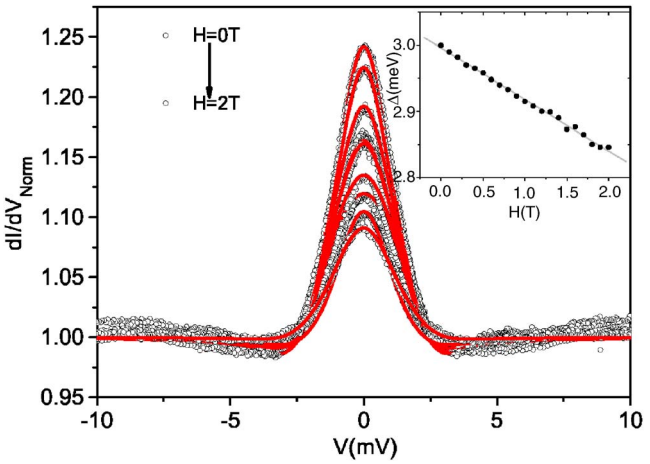

FIG. 6. (Color online) Magnetic field dependence of the normalized dI/dV vs V characteristics at $T=4.2$ K from 0 to 2 T (dots) for the spectra of Fig. 2(b). The full lines are the corresponding theoretical fittings. In the inset the magnetic field dependence of the energy gap is reported.

conducting and magnetic order is an important key for understanding the behavior of the Ru-1212 system. Coexistence of superconductivity and antiferromagnetism is found among cuprates, however it is a common belief that ferromagnetism and superconductivity are mutually excluding orders. Recently, it has been found that in conventional superconductor/ferromagnetic (S/F) structures, proximity effect gives rise to an oscillatory behavior of the superconducting T_c as a function of the thickness of the F layer.[25,26] There are conditions for which a change of sign of the order parameter occurs, producing the π-junction phenomenon.[27] In addition to this, a dramatic suppression of the amplitude of the order parameter is expected for high T_c superconductors in close contact with a ferromagnetic material[28] and various examples of anomalous temperature behavior are found in the literature. Gapless superconductivity can be achieved, that can induce a sublinear temperature dependence of the superconducting energy gap. In the Ru-1212 system, it has been proved that the RuO_2 planes are conducting, however these do not develop superconductivity at any temperature.[29] By means of different experimental techniques, it has been inferred that a large fraction of the charge carriers is not condensed in the superconducting state even at low temperatures.[29] Both findings are consistent with a reduced value of the $2\Delta/(k_B T_c)$ ratio in this compound.

In Fig. 5 we also report (right hand scale) the temperature evolution of the height of the ZBCP normalized to its value at $T=4.2$ K. It is worth noticing that $G_{NS}(V=0,T)$, as directly measured from the experiments, and $\Delta(T)$, as inferred from the theoretical fittings, show a similar scaling with temperature. This correspondence is easily verified for $Z=0$ in case of a *s-wave* superconductor, however it is quite a new result since it has been found for intermediate barriers and unconventional symmetry of the superconducting order parameter.

VI. MAGNETIC FIELD DEPENDENCE OF THE CONDUCTANCE SPECTRA

As we already observed, one of the most interesting features of the Ru-1212 is the coexistence of the superconducting phase and magnetic order. Indeed, from nuclear magnetic resonance[30,31] and magnetization[32] measurements, it has been found that in this compound ruthenium occurs in a mixed valence state Ru^{4+}, Ru^{5+} with some higher Ru^{5+} concentration. The RuO_2 planes, from one side, act as charge reservoir for the superconducting CuO_2 planes, on the other hand, as observed in Muon spin rotation (μSR) experiments,[8] they show quite homogeneous ferromagnetic order below T_c. A weak interaction between the two order parameters, ferromagnetism in the RuO_2 planes and superconductivity in the CuO_2 planes, has been suggested and recently several experiments appear to confirm this hypothesis.[29] Despite the huge experimental and theoretical efforts focused on the study of the interplay between superconductivity and magnetism, to the best of our knowledge no spectroscopic studies in magnetic field of the superconducting order parameter in Ru-1212 have been reported in literature so far.

In Fig. 6 we show the PCAR spectra measured by applying an external magnetic field, parallel to the tip, with intensity H varying from 0 to 2 T. The dI/dV vs V curves refer to the contact reported in Fig. 2(b). A reduction of the ZBCP for increasing magnetic fields is observed, that in first approximation can be reproduced by a phenomenological approach. Indeed, addressing the problem of the magnetic field dependence of the conductance characteristics in nonconventional superconductors is quite a difficult task and a complete treatment of PCAR spectroscopy in magnetic field would require the use of an appropriate density of states in calculating the BTK expression for the reflection and transmission coefficients at the N/S interface. Due to the lack of an analytical model, Miyoshi, Bugoslavsky, and Cohen[33] presented a two fluid model to reproduce the effect of normal vortex cores in PCAR junctions in conventional superconductors, assuming that the contact area contains multiple randomly distributed individual junctions (non-Sharvin regime[14]). These authors propose a simplified expression for the conductance, written as a sum of normal and superconducting channels

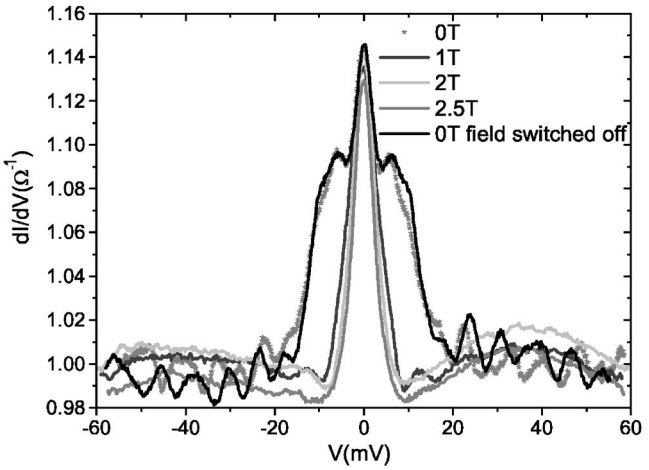

FIG. 7. Normalized conductance curves for the contact of Fig. 2(e) measured at $T=4.2$ K in magnetic field up to 2.5 T. When the field is switched off, the original spectra are recovered.

$$G_{NS_{tot}}(V) = (1-h)G_{NN} + hG_{NS}(V),$$

where $h=H/H_{c_2}$ and H_{c_2} is the critical field. This approach, however, cannot be applied to our experiments since we deal with polycrystalline, unconventional superconductor, exhibiting internal magnetic ordering. In this case, the magnetic induction B is not simply proportional to the external magnetic field H and as a consequence the density of vortices is not linearly related to H.

An alternative way to perform a theoretical fitting is obtained by using an additional pair breaking parameter to simulate the effect due to the magnetic field.[34,35] In this case, the total broadening effect Γ is considered as the sum of two terms: $\Gamma=\Gamma^{Dynes}+\Gamma^{ext}$ where Γ^{Dynes} is the intrinsic broadening due to the quasiparticle lifetime, as used in the previous fittings, while Γ^{ext} mimics the pair breaking effect due to the external applied magnetic field. The curve at $H=0$ T [see Fig. 2(b)] has been fitted by using the *d-wave* modified BTK model with $\Delta=3.0$ meV. For increasing magnetic fields we keep constant, in the numerical computation, the strength of the barrier $Z=0.9$, the orientation angle $\alpha=0.51$ and the intrinsic $\Gamma^{Dynes}=0.7$ meV, while varying only two parameters: the energy gap Δ and the magnetic field effect Γ^{ext}. We observe that the best theoretical fittings (solid lines in Fig. 6) satisfactorily reproduce for any field both the height and the amplitude of the measured spectra. In the inset, we report the magnetic field dependence of the superconducting energy gap (dots) as extracted from the theoretical fittings. The amplitude of the energy gap reduces linearly for H up to 2 T and by a linear extrapolation of the data, we find that the energy gap disappears at about $H^{ext}\simeq 30$ T, consistently with the estimated critical field reported in Ref. 11.

We have also studied the effect of the magnetic field on the conductance characteristics of the junctions showing wider ZBCP, that are formed by two junctions in series. In Fig. 7 we report the dI/dV vs V curves measured up to 2.5 T for the contacts of Fig. 2(e). In this case, we observe that the conductance curves dramatically change with the application of the magnetic field. As discussed in the previous section, the Josephson current due to the intergrain coupling is immediately suppressed by the magnetic field, modifying the spectra towards the narrower, nonstructured, triangular shape of the ZBCP. In addition to this, the oscillatory behavior of the background, due to the intergrain coupling, disappears in magnetic field. Remarkably, for the junctions of both Figs. 6 and 7 the peculiar features of the spectra, together with the normal junction resistance, are recovered when the magnetic field is switched off, and no hysteresis is found for increasing/decreasing fields.

VII. CONCLUSIONS

We have analyzed the PCAR conductance spectra obtained in superconducting $RuSr_2GdCu_2O_8$ (Ru-1212) polycrystalline pellets. All the conductance curves at low temperatures show a zero bias conductance peak that decreases for increasing temperatures and disappears at the local critical temperature $T_c^l\simeq 30$ K of the superconducting grain in contact with the Pt–Ir tip. The triangular shape of all the measured spectra has been modeled by using a modified BTK model for a *d-wave* symmetry of the superconducting order parameter. This finding suggests a closer similarity of the Ru-1212 system to the high T_c cuprate superconductors rather than to the magnetic ruthenate Sr_2RuO_4 compound. However, the remarkably low values of the energy gap $\Delta=(2.8\pm0.2)$ meV and of the ratio $2\Delta/k_BT_c\simeq 2$ indicate major differences between the Ru-1212 and the high T_c cuprates. We speculate that the presence of ferromagnetic order within the superconducting phase results in an effective reduction of the energy gap. We have also demonstrated that, when dealing with granular samples, intergrain coupling effects can play a predominant role. In some cases, an intergrain Josephson junction in series with the point contact junction is formed. Taking into account this feature as well, all conductance spectra have been properly modeled by considering a *d-wave* symmetry of the order parameter, with consistent values of the amplitude of the energy gap.

By fixing all the fitting parameters to their values at the lowest measured temperature, and by varying Δ, the temperature dependence of the energy gap has been extracted from the conductance characteristics of a very stable junction. We have found that the energy gap exhibits a sublinear dependence in temperature. The magnetic field behavior of the spectra has also been studied, showing a linear reduction of the energy gap for fields up to 2 T, from which a critical field $Hc_2\sim 30$ T is inferred. We have found that both the superconducting features and the normal background in the conductance spectra do not show any hysteresis in magnetic field. These observations seem to suggest a weak coupling between the superconducting and magnetic order parameter.

Our analysis may be helpful for a deeper understanding of the mechanisms enabling high temperature superconductivity, and its interplay with magnetic order in unconventional superconductors like rutheno cuprates.

The authors thank Y. Maeno and Y. Tanaka for helpful discussions and F. Vicinanza for the technical support.

[1] A. M. Duif, A. G. M. Jansen, and P. Wyder, J. Phys.: Condens. Matter **1**, 3157 (1989).
[2] A. F. Andreev, Zh. Eksp. Teor. Fiz. **46**, 1128 (1964).
[3] G. Deutscher, Rev. Mod. Phys. **77**, 109 (2005).
[4] L. Bauernfeind, W. Widder, and H. F. Braun, Physica C **254**, 151 (1995).
[5] T. Nachtrab, C. Bernhard, C. Lin, D. Koelle, and R. Kleiner, cond-mat/0508044 (unpublished).
[6] C. Bernhard, J. L. Tallon, E. Brücher, and R. K. Kremer, Phys. Rev. B **61**, R14960 (2000).
[7] J. W. Lynn, B. Keimer, C. Ulrich, C. Bernhard, and J. L. Tallon, Phys. Rev. B **61**, R14964 (2000).
[8] C. Bernhard, J. L. Tallon, Ch. Niedermayer, Th. Blasius, A. Golnik, E. Brücher, R. K. Kremer, D. R. Noakes, C. E. Stronach, and E. J. Ansaldo, Phys. Rev. B **59**, 14099 (1999).
[9] G. E. Blonder, M. Tinkham, and T. M. Klapwijk, Phys. Rev. B **25**, 4515 (1982).
[10] S. Kashiwaya and Y. Tanaka, Rep. Prog. Phys. **63**, 1641 (2000).
[11] C. Attanasio, M. Salvato, R. Ciancio, M. Gombos, S. Pace, S. Uthayakumar, and A. Vecchione, Physica C **411**, 126 (2004).
[12] M. Prester, E. Babić, M. Stubičar, and P. Nozar, Phys. Rev. B **49**, 6967 (1994).
[13] M. R. Cimberle, M. Tropeano, M. Feretti, A. Martinelli, C. Artini, and G. A. Costa, Semicond. Sci. Technol. **18**, 454 (2005).
[14] Y. Sharvin, Zh. Eksp. Teor. Fiz. **48**, 984 (1965) [Sov. Phys. JETP **21**, 655 (1965)].
[15] R. C. Dynes, V. Narayanamurti, and J. P. Garno, Phys. Rev. Lett. **41**, 1509 (1978).
[16] M. Grajcar, A. Plecenik, P. Seidel, and A. Pfuch, Phys. Rev. B **51**, 16185 (1995).
[17] L. Shan, H. J. Tao, H. Gao, Z. Z. Li, Z. A. Ren, G. C. Che, and H. H. Wen, Phys. Rev. B **68**, 144510 (2003).
[18] F. Giubileo, M. Aprili, F. Bobba, S. Piano, A. Scarfato, and A. M. Cucolo, Phys. Rev. B **72**, 174518 (2005).
[19] P. A. Lee, J. Appl. Phys. **42**, 325 (1971).
[20] T. Van Duzer and C. W. Turner, *Principles of Superconductive Devices and Circuits* (Arnold, London, 1981).
[21] A. Barone and G. Paternò, *Physics and Applications of the Josephson Effect* (Wiley, New York, 1982).
[22] A. M. Cucolo, Physica C **305**, 85 (1998).
[23] G. A. Ummarino, A. Calzolai, D. Daghero, R. S. Gonnelli, V. A. Stepanov, R. Masini, and M. R. Cimberle, cond-mat/0309553 (unpublished).
[24] Y. Dagan, R. Krupke, and G. Deutscher, Phys. Rev. B **62**, 146 (2000).
[25] A. I. Buzdin and M. V. Kuprianov, JETP Lett. **52**, 487 (1990).
[26] J. S. Jiang, D. Davidovic, D. H. Reich, and C. L. Chien, Phys. Rev. Lett. **74**, 314 (1995).
[27] W. Guichard, M. Aprili, O. Bourgeois, T. Kontos, J. Lesueur, and P. Gandit, Phys. Rev. Lett. **90**, 167001 (2003).
[28] P. S. Luo, H. Wu, F. C. Zhang, C. Cai, X. Y. Qi, X. L. Dong, W. Liu, X. F. Duan, B. Xu, L. X. Cao, X. G. Qiu, and B. R. Zhao, Phys. Rev. B **71**, 094502 (2005).
[29] M. Požek, A. Dulčić, D. Paar, A. Hamzić, M. Basletić, E. Tafra, G. V. M. Williams, and S. Krämer, Phys. Rev. B **65**, 174514 (2002).
[30] K. I. Kumagai, S. Takada, and Y. Furukawa, Phys. Rev. B **63**, 180509(R) (2001).
[31] Y. Tokunaga, H. Kotegawa, K. Ishida, Y. Kitaoka, H. Takagiwa, and J. Akimitsu, Phys. Rev. Lett. **86**, 5767 (2001).
[32] A. Butera, A. Fainstein, E. Winkler, and J. Tallon, Phys. Rev. B **63**, 054442 (2001).
[33] Y. Miyoshi, Y. Bugoslavsky, and L. F. Cohen, Phys. Rev. B **72**, 012502 (2005).
[34] Yu. G. Naidyuk, R. Häusslera, and H. V. Löhneysenet, Physica B **218**, 122 (1996).
[35] R. S. Gonnelli, D. Daghero, A. Calzolari, G. A. Ummarino, V. Dellarocca, V. A. Stepanov, J. Jun, S. M. Kazakov, and J. Karpinski, Phys. Rev. B **69**, 100504(R) (2004).